High energy γ rays from $^{14}N + {}^{nat}Ag$ at 35 MeV/nucleon

S. J. Luke and R. Vandenbosch
Nuclear Physics Laboratory, GL-10, University of Washington, Seattle, Washington 98195

W. Benenson, J. Clayton,* K. Joh, D. Krofcheck,† T. K. Murakami,‡
and J. D. Stevenson*
National Superconducting Cyclotron Laboratory, Michigan State University, East Lansing, Michigan 48824
(Received 16 September 1991; revised manuscript received 26 October 1992)

The absolute cross section and angular distributions for γ-ray production in the reaction $^{14}N + {}^{nat}Ag$ at 35 MeV/nucleon have been measured. Calculations of the expected γ-ray yield using an enhanced version of the nucleon exchange transport model have been performed. It has been observed that use of a sharp ground state momentum distribution in the γ-ray calculations does not lead to reproduction of the experimental yields. Diffuse momentum distributions have been incorporated into the model, and the calculations with these momentum distributions give good agreement with experimental yields. Similar calculations have been performed for the production of preequilibrium neutrons and protons for the same system.

PACS number(s): 25.70.−z

I. INTRODUCTION

There has been a great deal of interest in the production of high energy γ rays in the collision of heavy ions in the last several years. This effort has been in both the experimental and the theoretical vein. References [1] and [2] give good reviews of the theoretical and experimental situation, respectively. The γ rays of interest are those which have energies greater than the giant dipole resonance (GDR) and have energies which are comparable to or greater than the energy per nucleon available in the projectile. It is this second feature which makes these "hard" photons interesting to nuclear dynamics. γ rays of this type would necessarily come early in the reaction process before much of the energy in the initial system is dissipated as heat in the dinuclear system, thereby giving us a picture of the early stages of the heavy ion reaction process [3].

Much of the early experimental and theoretical effort was directed towards the determination of the mechanism for the production of these high energy photons. The first generation experiments were crude by present standards and led to interesting conclusions. Alamanos *et al.* [4] measured the angular distribution and singles yield of high energy γ rays from ^{14}N + Ni at 35 MeV/nucleon. The measured angular distribution had a dipole shape leading Vasak [5] to conclude that the γ rays were produced by a collective bremsstrahlung mechanism. Subsequent experiments have not supported this intepretation for the production mechanism of high energy γ rays. It is presently accepted that high energy γ rays from intermediate energy heavy ion collisions arise from incoherent nucleon-nucleon collisions [1]. There are two strong pieces of evidence for this thesis, namely, the analysis of the angular distribution of the γ rays produced in these collisions and the systematics of the γ-ray yields as a function of bombarding energy and system mass. The velocity of the source from which the radiation arises can be deduced from the fore-aft anisotropy in the laboratory frame assuming a reflection symmetric angular distribution in the source frame. This is discussed in more detail in Sec. III B.

One successful systematic of γ-ray production in heavy ion collisions is the so-called "equal participant" model [6]. This model assumes that the amount of γ-ray yield is proportional to the number of first chance proton-neutron collisions in the "participant zone." The integrated yield above a certain γ-ray energy, say, E_{min}, is assumed to be given by

$$\sigma_\gamma[E_\gamma > E_{\min}] = \sigma_R \langle N_{pn} \rangle P^\gamma_{pn}. \quad (1)$$

$\langle N_{pn} \rangle$ is the average number of first-chance proton-neutron collisions in the participant zone, and σ_R is the total reaction cross Section. Finally, P^γ_{pn} is the probability to produce a γ ray per proton-neutron collision. This has been shown to have a simple projectile velocity dependence for a wide variety of systems [7, 8]. This model has been able to systematize the yields of high energy γ rays for a large number of systems at beam energies above 20 MeV/nucleon [7, 1]. A nucleon exchange transport model calculation has shown that the high energy γ rays resulting from nucleon-nucleon bremsstrahlung in heavy ion collisions arise primarily from first-chance pn colli-

*Present address: Science Applications International Corp., Santa Clara, CA 95054.
†Present address: Lawrence Livermore National Laboratory, Livermore, CA 94550.
‡Present address: Department of Physics, Tokyo Institute of Technology, Oh-okayama, Meguro, Tokyo, 152 Japan.

sions. So the success of the "equal participant" model depends only on the additional validity of the geometric factors in defining the number of first-chance collisions in the participant zone.

The goal of the present study was to measure inclusive γ-ray yields and angular distributions for a system which satisfied two conditions. First, we wanted to be at a high enough bombarding energy so that we could be confident that the production mechanism was primarily from a nucleon-nucleon bremsstrahlung process with little contamination from compound nuclear processes. Second, we wanted to obtain γ-ray emission data for a system for which preequilibrium neutron (and possibly preequilibrium proton) inclusive data already existed. This was motivated by the fact that the production mechanism for hard nucleons and hard photons should be intimately connected [9, 10]. Both of these constraints were satisfied in the system ^{14}N + ^{nat}Ag at 35 MeV/nucleon.

Sections II and III describe the details of our measurement of the photon yields for this system, while Sec. IV describes our calculations for the expected yield of both hard photons and nucleons.

II. EXPERIMENT

High energy γ-ray production cross sections and angular distribution data have been measured for the system ^{14}N + ^{nat}Ag at 35 MeV/nucleon. The $^{14}N^{+5}$ beam was obtained at the National Superconducting Cyclotron Laboratory (NSCL) at the Michigan State University. Two detector systems were used for the measurement of the high energy γ rays: a large volume BaF_2 scintillator detector and a Čerenkov range telescope [11, 12]. A fairly complete angular distribution was obtained with measurements being made at seven angles between 30° and 150°.

The ^{14}N beam was delivered to the "neutron" beam line in the S320 spectrometer vault at the NSCL. The beam current was kept between 1 and 3 particle nA depending on the angle of the BaF_2 detector to keep the counting rate in the BaF_2 relatively constant. The Ag target was of natural composition and was 52 mg/cm^2 thick. This thickness led to a loss of 24 MeV in the target for the 490 MeV $^{14}N^{+5}$ ions. The target was mounted in a cylindrical beam tube which introduced a slight asymmetry in the attenuation of the γ rays at different angles. The effect of this different attenuation was very small though, being no greater than 2% in the γ-ray energy range of interest. The position of the beam was checked periodically by means of a scintillator placed in the target position. Absolute beam normalization was accomplished by means of a Faraday cup.

A. Čerenkov detector

The construction and performance of the Čerenkov detector have been discussed in detail elsewhere [13, 14]. The detector consists of a stack of eight lucite sheets doped with a wave shifter so that the Čerenkov light produced is absorbed and subsequently emitted in the visible range. A phototube was attached to the top and bottom of each Čerenkov element to collect the Čerenkov light produced. The overall depth of the Čerenkov detector was 34.29 cm, which is one radiation length for electrons in lucite.

In front of the first Čerenkov element was an active BaF_2 convertor. This convertor was 0.63 cm thick and had an active area of 100 cm^2 (10 cm × 10 cm); this area defined the geometry of the Čerenkov detector. Plastic anticoincidence paddles were placed in the front, back, and at the sides of the Čerenkov detector. These anticoincidence paddles were used to reject cosmic rays, which are a major source of background in γ-ray measurements. A graphite absorber was also placed in front of the Čerenkov detector to attenuate the energy of charged particles produced in the reaction.

The absolute energy scale is derived from the range table for electrons traversing through lucite. The absolute efficiency of the Čerenkov detector basically depends on the efficiency of the BaF_2 convertor to produce a e^-e^+ pair and is fairly flat for photon energies greater than 80 MeV. The absolute efficiency of the Čerenkov detector has been measured previously at the University of Illinois Tagged Photon Facility [14], and it is this experimentally measured efficiency which was used in the analysis of the present work.

B. BaF_2 detector

BaF_2 was chosen as a detector for high energy γ rays because of its superior timing characteristics, its high density, and an energy resolution only 30% worse than NaI [15, 16]. The detector itself was a 12.7 cm × 22.86 cm BaF_2 cylinder made by optically coupling two 12.7 cm × 11.43 cm cylindrical pieces together. Plastic anticoincidence paddles were placed on the top, at the sides and in front of the BaF_2 detector to reject cosmic-ray events and charged particles produced by the beam. A 20.32-cm-thick nylon absorber was placed in front of the BaF_2 crystal to attenuate the high energy charged particles and neutrons produced in the reaction. The γ rays were collimated to the rear face of the BaF_2 crystal by means of a 10-cm-thick lead collimator. The crystal was viewed by a single 5.08 cm quartz window R2250 phototube manufactured by the Hamamatsu Corporation.

The BaF_2 energy calibration was obtained using a Pu-Be source (E_γ = 4.4 MeV), the reaction ^{14}N + ^{12}C → γ + X^*, where X^* is an excited ^{13}C or ^{13}N produced by single nucleon transfer in either case resulting in a 15.1 MeV γ ray, and the peak produced by cosmic rays in the reject spectrum of the BaF_2 at 84.5 MeV. The efficiency of the BaF_2 was not obtained experimentally, but was calculated using the Monte Carlo code GEANT [17]. The calculated efficiency was found to be relatively flat above 20 MeV. Little is known about the response function of this BaF_2 for γ-ray energies between 20 and 75 MeV, though the response function to photons for this detector has been recently measured between 75 and 200 MeV [18]. Since the response of the detector is not well known in the present region of interest, no attempt has been made to fold the response function into the calcu-

lations described in Sec. IV. This could lead to an error of approximately 1 MeV in the calculated slope parameter [2].

C. Data acquisition and analysis

1. Data acquisition

The Čerenkov detector and the BaF_2 detector took data in singles mode. Events from the Čerenkov detector were processed as if there was an AND signal reflecting a coincidence between the convertor and the first two Čerenkov elements. This AND served as the start for each Čerenkov element charge sensitive ADC, as well as the start for the TDC which timed the Čerenkov detector against the cyclotron rf. The AND requirement in the Čerenkov detector set a threshold of about 10 MeV for the detection of γ rays, but we did not use any data below 20 MeV. The BaF_2 arm of the master event trigger was simply the fast component of the signal from the scintillator, while the integration of the slow component of the BaF_2 yielded the BaF_2 energy signal. The detectors were timed against the cyclotron rf to help discriminate against slowly moving charged particles and neutrons.

2. Data analysis

The data were analyzed at the University of Washington using the analysis code MUSORT. The analysis of the BaF_2 data was fairly straightforward. It involved sorting the accept γ-ray energy (those events which did not have a plastic veto signal associated with them) versus time of flight into two-dimensional spectra. Two-dimensional gates were then put around the prompt γ-ray peak to discriminate against neutrons produced in the reaction. This γ-ray/neutron discrimination was done in two dimensions to guard against possible time drifts in the time of flight spectrum. Neutrons proved to be the major source of background, especially at forward angles, and as a consequence no BaF_2 data forward of 75° were used.

The analysis of the Čerenkov data was a little more involved. First, the response of each Čerenkov element had to be determined. This was done using the cosmic-ray muon runs. Cosmic-ray muons were allowed to traverse the entire Čerenkov detector by demanding an AND between the front and back plastic anticoincidence paddles. This gave us the response of each element to fast particles, which is the same for all particles with $\beta > 0.2$. The spectrum for each Čerenkov element was fit with a Gaussian to find the centroid of the peak for a particle going through the entire element. Using the centroids we obtained software gain factors to position the peak of each spectrum in a specific channel. The energy of the initial γ ray could then be determined by reconstruction, on an event by event basis, from the ranges of the electrons and the positrons in the Čerenkov stack. The range of the electrons are determined by comparing the position of the peak in each element with that of a particle which traverses the entire element. Once the software gain factors had been determined, the data were sorted into two-dimensional energy vs time of flight spectra from which gates for the γ rays were determined. The data were sorted again to yield the final γ-ray spectra. The data from the Čerenkov detector were fairly clean, due mainly to the nature of the detector and the trigger condition.

III. RESULTS

A. Cross sections

Figure 1 shows the 90° energy spectrum of γ rays produced in the reaction ^{14}N + Ag at 35 MeV/nucleon. The shape of the spectrum suggests that there are two sources for the γ rays which are produced. These two sources are most probably statistical decay of the GDR and γ-ray production through a nucleon-nucleon bremsstrahlung mechanism. The data were fit with a function which was the sum of two exponentials. The solid line is the result of the two-exponential fit, and the dotted line is the exponential component with the steepest slope parameter, while the dashed line is the component with the flatter slope parameter. The former is assumed to arise from the tail of the GDR. We fit the inclusive data at each angle and obtained average values of 3.76±0.03 and 10.79±0.07 for the two slope parameters. The fits were done to the Čerenkov data only, since there was usable data at all angles from the Čerenkov detector.

The integrated yield above 30 MeV at 90° is 0.51 mb/sr. Using the prescription of the equal participant model discussed in Sec. I, we get a value for P^{γ}_{np} of 5.6 $\times$ 10^{-5}, which is consistent with systematics [7]. This supports the assumption that the production mechanism for these γ rays is nucleon-nucleon bremsstrahlung.

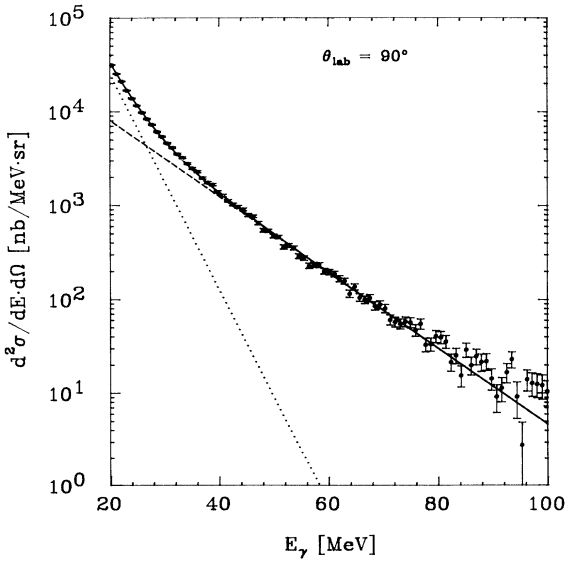

FIG. 1. 90° inclusive cross section for the production of high energy γ rays from 35 MeV/nucleon ^{14}N incident on ^{nat}Ag, using the Čerenkov detector. The solid line is the result of a fit to two exponentials. The dashed and the dotted lines are the components of the fit.

B. Angular distributions

Angular distributions for the γ rays produced in this reaction can be obtained by integrating the γ-ray yield over a selected energy region. Figure 2 shows the integrated yield for high energy photons above a γ-ray energy of 40 MeV in the laboratory frame. The angular distribution is very forward peaked with $\sigma(30°)/\sigma(150°)$ equal to 4.2. The errors which are shown in this figure are statistical errors and depend mostly on the size of the error at the lower energy end point, in this case 40 MeV. The solid line in Fig. 2 is the best fit to the angular distribution data assuming that the angular distribution for photon production in the source frame has a shape which has a $\sin^2\theta$ term, plus an isotropic term. The dashed line is the best fit to the data assuming the source angular distribution has a $\sin^2\theta\cos^2\theta$, a $\sin^2\theta$ term, and an isotropic term. The fit function is [2]

$$\frac{d^2\sigma_{\rm lab}}{dE\,d\Omega}[E_\gamma] = C_{\rm norm} f(\theta_{\rm lab}) e^{-E_{\rm low}\gamma(1-\beta\cos\theta_{\rm lab})/E_0}, \tag{2}$$

where

$$f(\theta_{\rm lab}) = \frac{\sin^2\theta}{\gamma^2\,(1-\beta\,\cos\theta_{\rm lab})^2}\left[\frac{15\,\alpha_{20}}{8\pi}\left(1-\frac{\sin^2\theta_{\rm lab}}{\gamma^2\,(1-\beta\,\cos\theta_{\rm lab})^2}\right)+\frac{3\,\alpha_{10}}{8\pi}\right]+\frac{\alpha_{00}}{4\pi}. \tag{3}$$

E_0 is the slope parameter for the emission in the source center of mass, $C_{\rm norm}$ is the overall normalization, and α_{00}, α_{10}, and α_{20} are the strengths of the isotropic, $\sin^2\theta$, and $\sin^2\theta\cos^2\theta$ terms, respectively. β is the velocity of the source, and γ is $1/\sqrt{1-\beta^2}$. The data from all seven angles are fitted simultaneously in a two-dimensional manner by the fit function in Eq. (2).

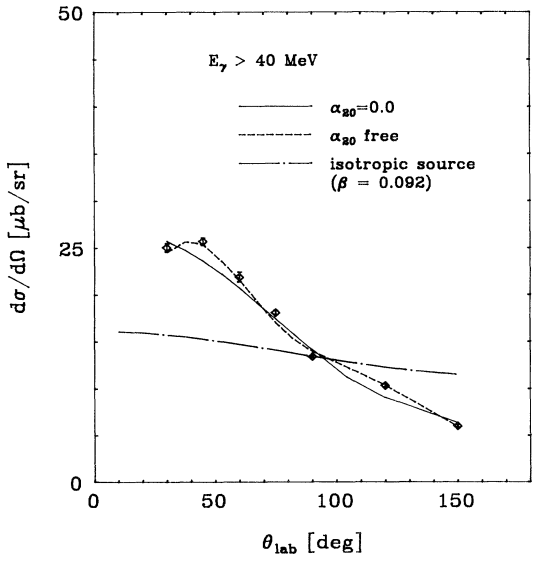

FIG. 2. Integrated yield of high energy γ rays above an energy of 40 MeV. The errors shown in the data are statistical. The solid line corresponds to the best fit to the data assuming a $\sin^2\theta$ plus isotropic angular distribution for the radiation in the source center of mass (see text). The dashed line corresponds to the best fit to the data assuming a $\sin^2\theta\cos^2\theta$ plus $\sin^2\theta$ plus an isotropic terms. The dash-dotted line represents the expectation for the integrated yield of γ rays being emitted isotropically from a source moving at the velocity of the compound nucleus ($\beta = 0.092$). This is normalized to the data at the 90° point.

The fit to the data gives the velocity of the source as well as the coefficients α_{00}, α_{10}, and α_{20}. If we let α_{20} be equal to zero, we find, for $E_\gamma > 40$ MeV, the velocity of the source to be 0.14 and the values for α_{10} and α_{00} to be 0.11±0.01 and 0.89±0.09, respectively. If we include the α_{20} term, we find that β is 0.13 and α_{20}, α_{10}, and α_{00} are 0.14±0.01, 0.30±0.02, and 0.56±0.05, respectively. The χ^2 per degree of freedom in these fits is 1.60 ($\alpha_{20} = 0$) and 1.44 (α_{20} included). The expectation for the source velocity from a nucleon-nucleon production mechanism, excluding coupling to the Fermi velocity and neglecting energy dissipation of the colliding nuclei (Sec. IV), is half the beam velocity. In the present case the β of the beam is 0.266, which corresponds to 0.133 in the nucleon-nucleon frame. The values for β which we obtain from both of these fits are consistent with the expectation for emission from the nucleon-nucleon frame.

The values for the components in the angular distribution fits are interesting. If we look at the fit to the data where the $\sin^2\theta\cos^2\theta$ term is excluded, the smallness of the $\sin^2\theta$ term compared to the isotropic term can be explained by Fermi motion smearing of the nucleon-nucleon frame. The γ-ray angular distribution is classically expected to have a $\sin^2\theta$ dependence in the emitter frame. The values for the coefficients in the fit including the $\sin^2\theta\cos^2\theta$ are both interesting and disturbing: interesting in the sense that this is the first time this term has been seen clearly in the data; disturbing because the magnitude of the $\sin^2\theta\cos^2\theta$ term is not understood. Nifenecker and Pinston [2] discuss the possible existence of such a term; using their prescription we calculate the ratio of α_{10}/α_{20} to be about 6:1 for our system. Our fit gives a value of about 2:1 for this ratio. It should be remembered, however, that the χ^2 per degree of freedom only changes from 1.60 to 1.44 with inclusion of the $\sin^2\theta\cos^2\theta$ term, and that the coefficient of this term depends strongly on the 90° measurement.

The dash-dotted line in Fig. 2 is the expectation of the integrated yield from a source emitting isotropically and moving at the velocity of the compound nucleus,

normalized to the data at 90°. Our angular distribution data is clearly inconsistent with significant contributions from compound nuclear emission.

IV. MODEL CALCULATIONS

Several models have been put forward to calculate the emission of high energy γ rays and hard nucleons in the collision of heavy ions. The way in which a model treats the underlying nuclear dynamics serves as a useful means by which to categorize the various models. Simulations which obtain the hard photon (and hard nucleon) emission probabilities by solving the Boltzmann-Uehling-Uhlenbeck (BUU) or Vlasov-Uehling-Uhlenbeck (VUU) [1] equations are one class of models. Another class of models are those using the Boltzmann-Master-Equation (BME) [21–23]. The model which we have used to perform our calculations is an extended version of the nucleon exchange transport model [10, 9], which has been modified lately [24] to include the emission of protons and neutrons as well as photons. This model was chosen because of its conceptual simplicity and its computational tractability as well as its success in describing the reaction dynamics of heavy ion collisions in the energy range between 10 and 40 MeV/nucleon.

A. Description of the model

The model which we use in this work is an extension of the nucleon exchange transport model used to study quasielastic and deeply inelastic collisions of heavy ions. (Hereafter this model will be referred to as the NET model.) The simulation of the reaction process proceeds as follows. The reacting nuclei are considered to be Fermi-Dirac gases composed of individual neutrons and protons. The isospin of the nucleons is kept track of throughout the collision process. The trajectory of the collision partners is governed by a Coulomb plus nuclear potential, plus one-body dissipation resulting from nucleon exchange. The colliding partners can overlap creating a neck. The amount of overlap of the nuclei and therefore the size of the neck depend on the impact parameter. Nucleons can be transferred between the collision partners. When such an exchange occurs the nucleon velocity due to Fermi momentum is boosted by the relative velocity of the two partners upon transfer. The propagation of the transferred nucleon through the receptor nucleus is followed. If the transferred nucleon collides with a nucleon with different isospin, the probability for the emission of γ rays via a np bremsstrahlung mechanism [9], of a *particular* energy, is calculated. The probability to have a nucleon-nucleon collision is based upon an isospin-averaged energy-dependent nucleon-nucleon scattering cross section. The probability for a particular collision to be an np collision reflects the 3 to 1 weighting of np compared to nn or pp collisions and the isospin composition of the system. The probability for the production of γ rays of a given energy depends on the final phase space availability of the scattered nucleons. If the phase space is open in the final state, then a γ ray can be produced. The emitted γ ray is assumed to be emitted randomly with a dipole distribution in the nucleon-nucleon center of mass, and it is then transformed into the laboratory frame. Because the photon interacts very weakly with the nuclear matter, it is assumed that the nucleus is transparent to the emitted photon and the γ ray leaves the nucleus unperturbed.

It should be noted that collisional bremsstrahlung is the only mechanism for producing γ rays in this work; and in the nonrelativistic limit for this bremsstrahlung production only the convection current enters. It has been shown that the meson exchange current contributes significantly to the bremsstrahlung rate in pn collisions [25], especially at high γ-ray and pn collision energies. The expectation is that the exchange current contribution will diminish at lower γ-ray and pn collision energies [26]. At most there is a 30% difference between calculations which include and ignore the exchange current effect on the elementary $np \rightarrow \gamma$ rate, in our kinematic regime [27]. Another possible bremsstrahlung mechanism which we have not included is bremsstrahlung from the mean field. The expectation is that this process will contribute a factor of 5–6 less than the collisional effects for our system in the γ-ray energy region between 30 and 60 MeV [28], but will be somewhat more important for γ rays with energy less than 30 MeV [29].

The algorithm for the emission of hard nucleons is very similar to that of the production of the high energy γ rays. A major difference is that the transferred nucleon need not collide with a nucleon in the receptor. It may escape without a collision, or it can collide with either neutrons or protons. After the collision probability is calculated, the final phase space is checked for availability, and if the final phase space is not Pauli blocked, the trajectory of the two nucleons is followed through the nucleus. In the journey of the nucleons from any collision point to the surface, secondary collisions and therefore rescatterings are allowed; at each point the collision probability is recalculated and the Pauli blocking is checked. When the nucleons reach the surface, the escape probability is determined by calculating the penetrability through a potential barrier associated with the nuclear surface. If the escaping nucleon is a neutron, after refraction at the surface it is assumed to proceed in a straight line path. If the escaping nucleon is a proton, it follows a Coulomb trajectory based upon the proton's interaction with the dinucleus [24].

We did two types of calculations with the NET model. We will call these the "default" calculation and the "enhanced" calculation. The default calculation assumes that the initially cold nuclei were sharp isotropic Fermi-Dirac gases. This type of calculation has been presented in the literature previously [9, 10]. In the enhanced version of the model described in detail elsewhere [19, 20], a *diffuse* Fermi-Dirac momentum distribution is used rather than a sharp momentum distribution [31–34]. This diffuse momentum distribution was motivated by the results of quasifree electron scattering experiments [35, 36] which show that the nucleon momentum distribution has a high-momentum component beyond the Fermi momentum in the sharp Fermi sphere picture. The "diffuseness" parameter for the momentum

distribution is determined by reproducing the slope of the experimental momentum distribution [20]. Inclusion of these momentum tails has two main consequences in the emission of hard photons and nucleons. The first consequence is the presence of nucleons with higher momentum components. This has the effect of "hardening" the spectra of emitted particles in the high energy region. The second consequence is that the diffuse momentum distribution has the effect of opening up the final state phase space, thereby reducing the Pauli blocking which results in an overall increase of emitted particles at all energies. A difficulty associated with this extension is that spurious emission of photons and nucleons can arise from the transfer of nucleons in the absence of relative motion between the projectile and target. A modest correction, typically 15% at the energies of interest, has been made in obtaining the results presented below.

B. Results of model calculations

1. *Results of calculations for γ-ray emission*

Figure 3(a) shows the result of calculations compared to our experimental data at 90°. The dashed line shows the results of the default calculation, while the solid line is the result of the calculation using a diffuse momentum distribution. Figure 3(a) clearly shows the effect of the inclusion of a diffuse momentum distribution discussed above. The overall increase of γ-ray yield is seen at all energies. The yield increases from about a factor of 2 at 40 MeV to an order of magnitude at 100 MeV. We are not able to reproduce the yield of γ rays below an energy of 40 MeV. The excess production of γ rays in this energy range is probably the result of production via statistical decay of excited nuclei produced in the reaction. These could arise either from statistical decay of heavy nuclei resulting from complete fusion of the projectile and target, in which case a small source velocity would be expected, or from the decay of excited projectilelike fragments from peripheral collisions, in which case a high source velocity would be expected. The latter process seems to dominate since a fit of the angular distribution for γ rays between 20 and 30 MeV yields a source velocity (β) of 0.15. This is significantly greater than that expected for the compound nucleus ($\beta = 0.031$) but less than the velocity of the beam ($\beta = 0.266$). We therefore attribute these γ rays to the tail of the GDR of projectilelike fragments. These fragments have a GDR centroid considerably higher in energy than that of heavy fusionlike fragments [30].

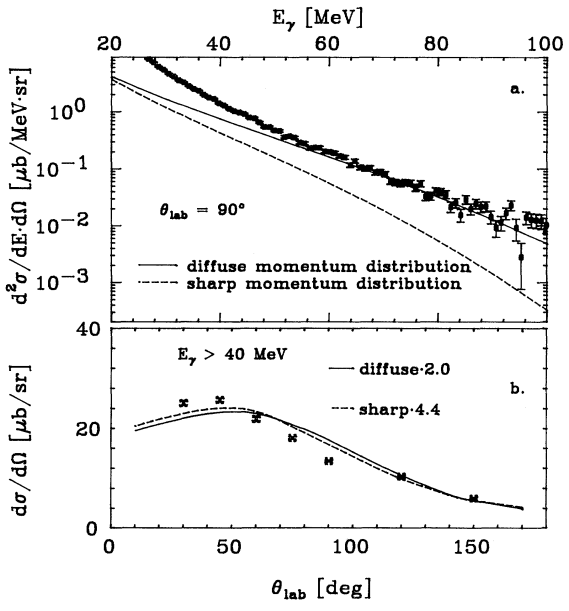

FIG. 3. Comparison of the experimental data with model calculations. (a) The 90° inclusive spectrum for hard photon production compared to model calculations. The dashed line is the result of the default calculation using the nucleon exchange transport model (see text). The solid line is the result of the calculation of the yield of hard photons using a diffuse momentum distribution in the nucleon exchange transport model. (b) The calculated energy integrated ($E_\gamma > 40$ MeV) angular distributions using both diffuse and sharp ground state momentum distributions. The experimental data are from the Čerenkov detector.

Figure 3(b) shows the results of the calculation of the angular distribution for the emission of high energy photons for γ rays with energy greater than 40 MeV, using both diffuse and sharp ground state momentum distributions. The calculations are normalized to the data at 30°, 90°, and 150°. This was necessary because we are unable to reproduce the experimental yield at 40 MeV. As this figure shows, both calculations reproduce the shape of the photon angular distributions fairly well. The calculation which uses a sharp momentum distribution has a slightly larger forward/backward asymmetry because there is less smearing due to the Fermi motion [19]. The calculated angular distribution is definitely forward peaked, but it is not forward peaked enough to reproduce the data.

2. *Results of calculations for nucleon emission*

In addition to calculating the γ-ray emission probability for the present reaction, we have also calculated the neutron and proton emission yields. The neutron calculations are compared to the experimental data [37] in Fig. 4, and the proton calculations are compared to the experimental data [38] in Fig. 5. There is less of a difference between the sharp and diffuse momentum distributions on the neutron and proton spectra as there was for the photon spectra. There is more extensive angular distribution data for neutrons than there is for protons, and so we are able to see how the model does at forward versus backward angles. At forward angles (in this case 31°) we reproduce the observed neutron spectra fairly well above 40 MeV with the calculation using a sharp ground state momentum distribution. The calculation using a diffuse ground state momentum distribution overpredicts the experimental yield by about 25–30 %. The situation at backward angles is very similar; the calculations using a sharp ground state momentum distribution

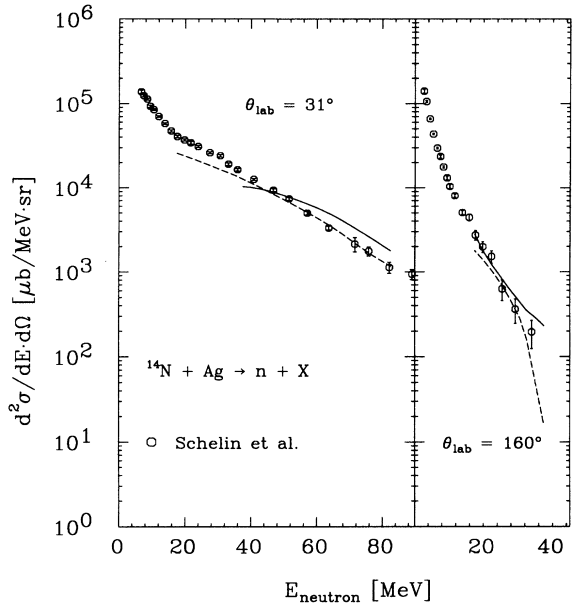

FIG. 4. Inclusive spectra of neutrons produced in the reaction ^{14}N + ^{nat}Ag at 35 MeV/nucleon. The data are from Schelin *et al.* [37]. The dashed line is the result of the default calculation of the hard neutron yield from the nucleon exchange transport model. The solid line is the result of the calculation using a diffuse momentum distribution in the nucleon exchange transport model.

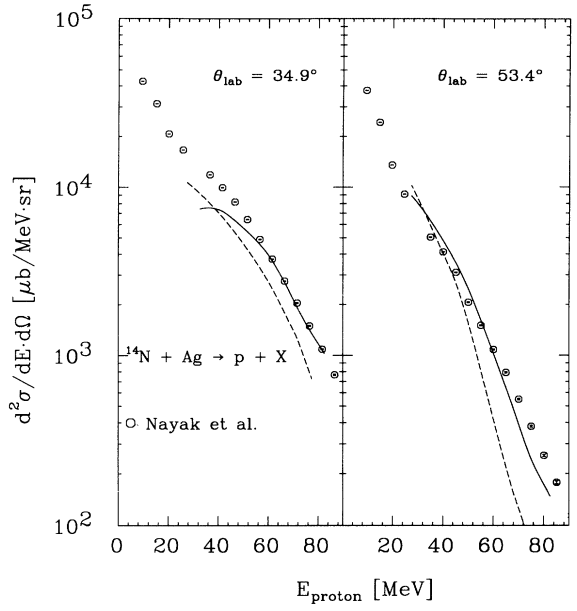

FIG. 5. Inclusive spectra of protons produced in the reaction ^{14}N + ^{nat}Ag at 35 MeV/nucleon. The data are from Nayak *et al.* [38]. The dashed line is the result of the default calculation of the hard proton yield from the nucleon exchange transport model. The solid line is the result of the calculation using a diffuse momentum distribution in the nucleon exchange transport model.

reproduce the data fairly well, while the calculation using a diffuse momentum distribution slightly overpredicts the experimental yield. The results of the calculations using the diffuse momentum distribution at backward angles are tenuous because the background correction becomes rather large.

The results of the calculated proton spectra using a diffuse ground state momentum distribution agree reasonably well with the experimental data at higher energies where evaporation decay from the composite nucleus and sequential decay of the projectilelike fragments are not important. The 53.4° spectrum is slightly overpredicted at low proton energies and somewhat underpredicted at high proton energies.

V. SUMMARY AND OUTLOOK

We have measured inclusive cross sections and angular distributions of high energy γ rays produced in the reaction ^{14}N + ^{nat}Ag at 35 MeV/nucleon. We have shown that the production mechanism for these γ rays is through a nucleon-nucleon bremsstrahlung process.

We also have performed calculations using the nucleon exchange transport model to compare with the experimental results. This model has no adjustable parameters. We have shown that it is necessary to include a diffuse momentum distribution in order to understand the yield of the γ rays produced in this reaction. Similar calculations were performed for the emission of preequlibrium neutrons and protons for the same system. The diffuse momentum distribution gives reasonable agreement with the experimental nucleon emission data at forward angles for particle energies where evaporative contributions are less important. Our present calculations do account for the "softness" of the observed neutron spectrum at 160°. However, this result should be taken cautiously because of the increased importance of the "background" calculations at backward angles. More backward angle data for protons would be highly desirable.

The present γ-ray data are particularly useful because they complete a data set for the emission of energetic products from one reaction. Thus for the first time one has available neutron, proton, and γ-ray data for the same system at the same bombarding energy. Comparison of the calculated γ-ray and nucleon spectra show that energetic photon emission is the most sensitive observable dependent on the nucleon momentum distribution. We feel that more of such data is needed in order to understand the reaction dynamics at the early stages of heavy ion collisions.

ACKNOWLEDGMENTS

We wish to thank Jørgen Randrup for his helpful suggestions and stimulating discussions. One of us (S.J.L.) wishes to thank Brian McLain for his patience with endless questions concerning various computer programs. S.J.L. and R.V. would like to thank the staff of the NSCL for their hospitality and their professional operation of the K500 cyclotron. This work was supported by Department of Energy Grant No. DE-FG06-90ER40537 and by National Science Foundation Grant No. PHY-89-13815.

[1] W. Cassing, V. Metag, U. Mosel, and K. Niita, Phys. Rep. **188**, 363 (1990).
[2] H. Nifenecker and J. A. Pinston, Prog. Part. Nucl. Phys. **23**, 271 (1989).
[3] W. Cassing, T. Biró, U. Mosel, M. Tohayama, and W. Bauer, Phys. Lett. B **181**, 217 (1986).
[4] N. Alamanos, P. Braun-Munzinger, R. F. Freifelder, P. Paul, J. Stachel, T. C. Awes, R. L. Ferguson, F. E. Obenshain, F. Plasil, and G. R. Young, Phys. Lett. B **173**, 392 (1986).
[5] D. Vasak, Phys. Lett. B **176**, 276 (1986).
[6] H. Nifenecker and J. P. Bondorf, Nucl. Phys. **A442**, 478 (1985).
[7] V. Metag, Nucl. Phys. **A482**, 159c (1988).
[8] V. Metag, Ann. Phys. (Leipzig) **48**, 121 (1991).
[9] J. Randrup and R. Vandenbosch, Nucl. Phys. **A490**, 418 (1988).
[10] J. Randrup and R. Vandenbosch, Nucl. Phys. **A474**, 418 (1987).
[11] K. Beard, W. Benenson, C. Bloch, E. Kashy, J. Stevenson, D. J. Morissey, J. van der Plicht, B. Sherrill, and J. S. Winfield, Phys. Rev. C **32**, 1111 (1985).
[12] J. Stevenson, K. B. Beard, W. Benenson, J. Clayton, E. Kashy, A. Lampis, D. J. Morissey, M. Samuel, R. J. Smith, C. L. Tam, and J. S. Winfield, Phys. Rev. Lett. **57**, 555 (1986).
[13] A. R. Lampis, Ph.D. thesis, Michigan State University, 1988.
[14] J. Stevenson *et al.* (in preparation).
[15] M. Laval, M. Moszyński, R. Allemand, E. Cormoreche, P. Guinet, R. Ordu, and J. Vacher, Nucl. Instrm. Methods A **206**, 169 (1983).
[16] K. Wisshak and Käppeter, Nucl. Instrm. Methods A **227**, 91 (1984).
[17] R. Brun, F. Bruyant, M. Maire, A. C. McPherson, and P. Zanarini, Geant, CERN Technical Report No. DD-EE-84-1, 1987.
[18] J. Clayton, W. Benenson, N. Levinsky, J. Stevenson, M. F. Mohar, E. Hallin, J. C. Bergstrom, H. S. Caplan, R. E. Pywell, D. M. Skopik, and J. M. Vogt, Nucl. Instrum. Methods A **305**, 116 (1991).
[19] S. J. Luke, Ph.D. thesis, University of Washington, 1992.
[20] S. J. Luke, R. Vandenbosch, and J. Randrup (in preparation).
[21] B. A. Remington, M. Blann, and G. F. Bertsch, Phys. Rev. Lett. **57**, 2909 (1986).
[22] B. A. Remington, M. Blann, and G. F. Bertsch, Phys. Rev. C **35**, 1720 (1987).
[23] B. A. Remington and M. Blann, Phys. Rev. C **36**, 1387 (1987).
[24] J. Randrup and R. Vandenbosch (unpublished).
[25] K. Nakayama, Phys. Rev. C **39**, 1475 (1989).
[26] U. Mosel (private communication).
[27] M. Schäfer, T. S. Biró, W. Cassing, U. Mosel, H. Nifenecker, and J. A. Pinston, Z. Phys. A **339**, 391 (1991).
[28] K. Nakayama and G. Bertsch, Phys. Rev. C **34**, 2190 (1986).
[29] R. Heuer, B. Müller, H. Stöcker, and W. Greiner, Z. Phys. A **330**, 315 (1988).
[30] C. A. Gossett, J. A. Behr, G. Feldman, J. H. Gundlach, M. Kicinska-Habior, and K. A. Snover, J. Phys. G Suppl. **14**, S267 (1988).
[31] S. J. Luke, R. Vandenbosch, W. Benenson, J. Clayton, K. Joh, D. Krofcheck, T. K. Murakami, and J. Stevenson, Bull. Am. Phys. Soc. **34**, 1818 (1989).
[32] S. J. Luke and R. Vandenbosch, University of Washington Nuclear Physics Laboratory Annual Report, 1990.
[33] J. Wile, S. S. Datta, R. T. deSouza, J. R. Huizenga, D. Pade, W. U. Schröder, and J. Tõke, Phys. Rev. Lett. **63**, 2551 (1989).
[34] K. Niita, University of Giessen report, 1991.
[35] A. Antonov, P. Hodgson, and I. Pertov, *Nucleon Momentum and Density Distributions in Nuclei* (Clarendon, Oxford, 1988).
[36] I. Sick, in *Momentum Distributions*, edited by R. N. Silver and P. E. Sokol (Plenum, New York, 1989).
[37] H. R. Schelin, A. Galonsky, C. K. Gelbke, L. Heilbronn, W. G. Lynch, T. Murakami, M. B. Tsang, X. Yang, G. Zhang, B. A. Remington, F. Deàk, A. Kiss, Z. Seres, and J. Kasagi, Phys. Rev. C **39**, 1827 (1989).
[38] T. Nayak, T. Murakami, W. G. Lynch, K. Swartz, D. J. Fields, C. K. Gelbke, Y. D. Kim, J. Pochodzalla, M. B. Tsang, H. M. Xu, F. Zhu, and K. Kwiatkowski, Phys. Rev. C **45**, 132 (1992).